crystals

MDPI

Article

Phosphogypsum Additive as Shrinkage-Reducing Agent in Ordinary Portland Cement-Based Mortar

Valdas Rudelis [1], Danutė Vaičiukynienė [2], Algirdas Augonis [2], Modestas Kligys [1,*] and Giedrius Girskas [1]

[1] Faculty of Civil Engineering, Vilnius Gediminas Technical University (VILNIUS TECH), Saulėtekio al. 11, 10223 Vilnius, Lithuania; valdas.rudelis@vilniustech.lt (V.R.); giedrius.girskas@vilniustech.lt (G.G.)
[2] Faculty of Architecture and Civil Engineering, Kaunas University of Technology, Studentų st. 48, 51367 Kaunas, Lithuania; danute.vaiciukyniene@ktu.lt (D.V.); algirdas.augonis@ktu.lt (A.A.)
* Correspondence: modestas.kligys@vilniustech.lt

Abstract

Phosphogypsum, a by-product of phosphate fertilizer production, has shown promising potential as a shrinkage-reducing additive in ordinary Portland cement-based mortar. The incorporation of low PG dosages (≤6%) enhances early hydration, slightly increases the hydration peak temperature, and promotes the formation of additional ettringite and bound-water-rich hydrates, contributing to improved early performance. PG also substantially reduces drying shrinkage—from 0.0397 mm/m (reference) to −0.1600 mm/m at 15% PG—through ettringite-induced expansion and pore refinement, demonstrating its effectiveness as a shrinkage-reducing agent. Thermal analysis (XRD/TG–DTA) confirms that PG modifies hydration chemistry by increasing low-temperature dehydration while reducing portlandite and carbonate phase formation due to clinker dilution. As a result, $Ca(OH)_2$ content decreases from 11.89 wt% for the reference mix to 8.55 wt% at 15% PG. However, higher PG levels (>9%) negatively affect strength: at 15% PG, flexural and compressive strength decrease by 38% and 47%, respectively, due to clinker dilution, excess ettringite, and unreacted gypsum. All compositions maintained durability levels corresponding to roughly 300–450 freeze–thaw cycles. Overall, PG effectively reduces shrinkage and alters hydration behavior while offering environmental benefits through industrial waste valorization. Nevertheless, high replacement levels compromise mechanical performance, underscoring the importance of optimizing PG dosage to balance shrinkage control, strength, and sustainability.

Keywords: phosphogypsum; shrinkage reducing additives; OPC-based mortar; dimensional stability

Check for updates

Academic Editor: Leonid Kustov

Received: 26 November 2025
Revised: 24 January 2026
Accepted: 27 January 2026
Published: 30 January 2026

Copyright: © 2026 by the authors. Licensee MDPI, Basel, Switzerland. This article is an open access article distributed under the terms and conditions of the Creative Commons Attribution (CC BY) license.

1. Introduction

Shrinkage deformation is a critical concern in the performance and durability of ordinary Portland cement (OPC) concrete. As concrete hardens and loses moisture, it undergoes volumetric changes that can lead to cracking, reduced mechanical integrity, and long-term deterioration. These shrinkage effects—primarily drying shrinkage and autogenous shrinkage—are influenced by factors such as cement composition, water–cement ratio, curing conditions, and admixture use [1,2].

In structural applications, uncontrolled shrinkage can compromise serviceability, increase maintenance costs, and shorten the lifespan of concrete elements [3]. Therefore, understanding and mitigating shrinkage deformation is essential for improving the reliability and sustainability of concrete infrastructure. Recent research has focused on the

use of shrinkage-reducing additives (SRAs), expansive agents like quicklime and Portland expanded cement, and fiber reinforcements to control shrinkage and enhance mechanical performance. These materials interact with the cement matrix in different ways—modifying hydration kinetics, altering pore structure, and improving crack resistance. Statkauskas et al. [4] investigated the effects of various SRAs on ordinary Portland cement (OPC) concrete. The study included organic compound-based SRA, quicklime, polypropylene fiber, and hemp fiber. The most effective shrinkage reduction was achieved with a combination of 2.5% quicklime and 1.5% SRA, resulting in up to 40.0% shrinkage reduction. However, all samples showed decreased compressive strength after 28 days of hydration. In [5], the influence of water-reducing agents on both drying shrinkage and autogenous shrinkage of cement mortar was investigated. Polycarboxylate superplasticizers exhibited the best dispersion performance and the highest sensitivity in modifying cement paste fluidity. The shrinkage reduction was explained by several synergistic mechanisms: delayed exothermic peak during hydration, lower surface tension of the pore solution, and reduction in both large and small capillary pores. Wang et al. [6] found that increasing SRA dosage in UHPC mortar reduced fluidity and delayed hydration, extending setting time and lowering early strength. Autogenous shrinkage dropped significantly at 0–2% SRA, and even 0.5% reduced drying shrinkage. Portland expanded cement improved early strength but raised autogenous shrinkage while reducing drying shrinkage at 25–50%. SEM analysis showed that higher SRA led to a looser microstructure with incomplete hydration products, reducing strength. The study in [7] reports early-age restrained shrinkage tests on OPC concretes containing polypropylene (PP) fibers. Increasing PP fiber volume fractions significantly delayed cracking by postponing the onset of restrained shrinkage, thereby improving crack resistance. Zuo et al. [8] found that combining low-heat Portland cement, MgO-based expansive agent, and SRA reduces concrete cracking risk. MgO-based expansive agent increases dynamic yield stress, plastic viscosity, and accelerates hydration, while SRA slows hydration and lowers hydration products. Despite this, SRA further raises static yield stress, correlating with hydrated particle surface area. In [9], the effect of a fatty-alcohol-based SRA under practical hydration and evaporation conditions was studied. The analysis showed that SRA increased the size of disk-shaped C-S-H agglomerates and more mesopores forming between or within these units as SRA content rose. These stable mesoporous structures reduced early-age drying shrinkage. Wan et al. [10] reported that shotcrete is more prone to shrinkage cracking than OPC concrete due to high cement content, small aggregate size, and accelerated early hydration. Increasing SRA dosage lengthened setting time and slightly reduced 1-day strength, but both autogenous and drying shrinkage decreased over 180 days. Microscopic analysis showed SRA delays early hydration with accelerators but has minimal long-term impact. The researchers in [11] investigated autogenous and drying shrinkage in precast recycled aggregate concrete. Recycled aggregates generally reduce autogenous shrinkage but increase drying shrinkage, with finer aggregates having a stronger effect. Higher parent concrete strength slightly affects autogenous shrinkage but significantly lowers drying shrinkage. While two-stage mixing has little impact, the equivalent volume mortar method markedly reduces both shrinkage types. Tutkun et al. [12] studied internal curing and its effect on shrinkage and cracking. Superabsorbent polymers effectively reduced autogenous and drying shrinkage by limiting early plastic strains. However, crack mapping revealed larger cracked areas with SAP use, higher curing water, and larger superabsorbent polymer particles, indicating that while shrinkage decreases, overall cracking behavior can vary. Another study [13] examined autogenous and drying shrinkage in UHPC and the role of internal curing using pre-saturated lightweight sand (LWS). A 40% LWS mix reduced autogenous shrinkage by 75% and increased internal relative humidity by 10% at 56 days, while also

cutting drying shrinkage by 26%. Restrained ring tests showed low cracking potential in all mixes, largely due to fibers bridging microcracks. Zhu et al. [14] evaluated precast member joint concrete (PMJC) with a mix of 0.38 water–binder ratio, 30% fly ash, 3% ultra-fine silica, 47.7% sand, 8% expansive agent, and 0.7% water reducer. The mix showed good workability for on-site construction, matched precast member strength, and provided ductility, stability, and minimal early shrinkage, meeting joint material requirements. Al-Alusi et al. [15] studied single-size expanded polystyrene-based lightweight concrete with waste plastic fibers. Expanded polystyrene reduced strength and increased shrinkage, while waste plastic fibers (0–1%) improved strength but declined beyond 1%. Waste plastic fibers (0.25–1.25%) lowered shrinkage versus the reference mix. Shrinkage peaked at 40–60 days, and then stabilized.

This study used phosphogypsum (PG) as a shrinkage-reducing additive, though few studies address PG for this purpose. Han-jitsuwan et al. [16] examined alkali-activated high-calcium fly ash paste using PG and dolomite as expansive additives. Replacing fly ash with 0–10% additives reduced drying shrinkage, shortened setting time, and increased strength. Higher liquid/binder ratios worsened shrinkage. Long-term strength declined with PG but improved with dolomite. Strength gains were linked to the formation of specific phases. Dolomite was more effective for shrinkage control and durability. Bakharev et al. [17] found that adding 6% gypsum by weight to alkali-activated slag reduced both autogenous and drying shrinkage due to ettringite formation, which acted as an expansive phase. Liu et al. [18] studied sodium silicate-activated slag with gypsum and OPC additives. Both additives significantly reduced drying shrinkage by forming expansive products such as ettringite and portlandite. Gypsum accelerated hydration, while OPC delayed initial setting. Blending 20% OPC with gypsum slightly improved flexural and compressive strength at 7 and 28 days.

Previous literature reviews revealed no evidence of phosphogypsum (PG) being used as a shrinkage-reducing agent in OPC systems. This study evaluates the effectiveness of PG in OPC mortar, aiming to determine optimal PG dosages that minimize shrinkage while maintaining or enhancing mechanical properties.

2. Materials and Methods

2.1. Characterization of Initial Materials

Portland cement (CEM I 42.5 R) was employed as the binder for producing OPC-based mortar. The chemical compositions of OPC and PG used in this study are summarized in Table 1. Based on XRF analysis, the main oxides in OPC include SiO_2 (20.0%), CaO (63.4%), Al_2O_3 (4.57%), Fe_2O_3 (3.46%), and MgO (3.71%). For PG, the predominant oxides are CaO (38.20%) and SO_3 (51.0%), which are consistent with values reported in previous studies [19].

Table 1. Oxide composition of initial materials, according to the XRF, wt%.

Oxides	SiO_2	CaO	Al_2O_3	Fe_2O_3	MgO	K_2O	P_2O_5	SO_3	Na_2O	F	LOI	Other
OPC	20.0	63.4	4.57	3.46	3.71	1.30	-	2.70	0.14	-	0.60	0.12
PG	0.97	38.2	0.12	0.05	0.05	0.69	0.30	51.0	0.09	0.18	6.55	1.80

Phosphogypsum (PG), a by-product generated during the production of phosphate fertilizers, represents one of the largest industrial waste streams worldwide and is currently underutilized despite its potential in construction applications. Chemically, PG is predominantly composed of calcium sulfate semi- or dihydrate ($CaSO_4 \cdot 0.5/2H_2O$), similar to natural gypsum. With a calcium sulfate content of up to 89%, PG corresponds to nat-

ural gypsum. However, its direct application in gypsum-based products is constrained by the presence of water-soluble phosphates and fluoride, impurities that can interfere with gypsum hydration reactions and retard setting and compromise long-term durability. In addition, PG often contains trace amounts of heavy metals and naturally occurring radionuclides, raising environmental and health concerns that necessitate careful handling and compliance with regulatory standards. In our previous study [20], the suitability of Lithuanian PG for construction was confirmed through radioactivity testing. High-resolution gamma spectrometry detected radionuclides (^{226}Ra, ^{228}Ra, ^{228}Th, ^{40}K, ^{210}Pb) all below clearance limits, and calculated activity indices that complied with regulatory standards, allowing its use in building materials. When PG is incorporated into OPC systems, phosphorus and fluoride present in PG tend to precipitate as insoluble calcium compounds [21]. In addition, phosphorus can be immobilized through sorption onto hydration products, particularly calcium silicate hydrates (C–S–H) and ettringite, which provide reactive sites for anion incorporation [22]. These mechanisms collectively contribute to the chemical stabilization of harmful species during cement hydration, thereby improving the compatibility of PG with cementitious systems.

Despite these limitations, recent research has explored strategies to incorporate PG into sustainable construction materials, such as its use as a supplementary additive in Portland cement binders, where it can contribute to improved dimensional stability and reduced shrinkage. The valorization of PG not only mitigates the environmental burden associated with its disposal, but also supports circular economy principles by converting industrial waste into value-added products.

Figure 1 illustrates the particle size distributions of the OPC and PG used in this study. For OPC, particle sizes ranged from 0.05 to 52.5 µm (Figure 1a). Two distinct peaks were observed in the distribution: one at 1.8 µm (representing 1.75% of particles) and another at 19.42 µm (2.14% of particles). The OPC particles exhibit a particle size distribution with $D_{10} \approx 0.96$ µm, $D_{50} \approx 5.57$ µm, and $D_{90} \approx 23.34$ µm. Overall, OPC exhibited a higher proportion of fine particles compared to PG. The particle size distribution of PG was as follows: $d_{10} \approx 0.74$ µm, $d_{50} \approx 4.63$ µm, and $d_{90} \approx 19.98$ µm (Figure 1b).

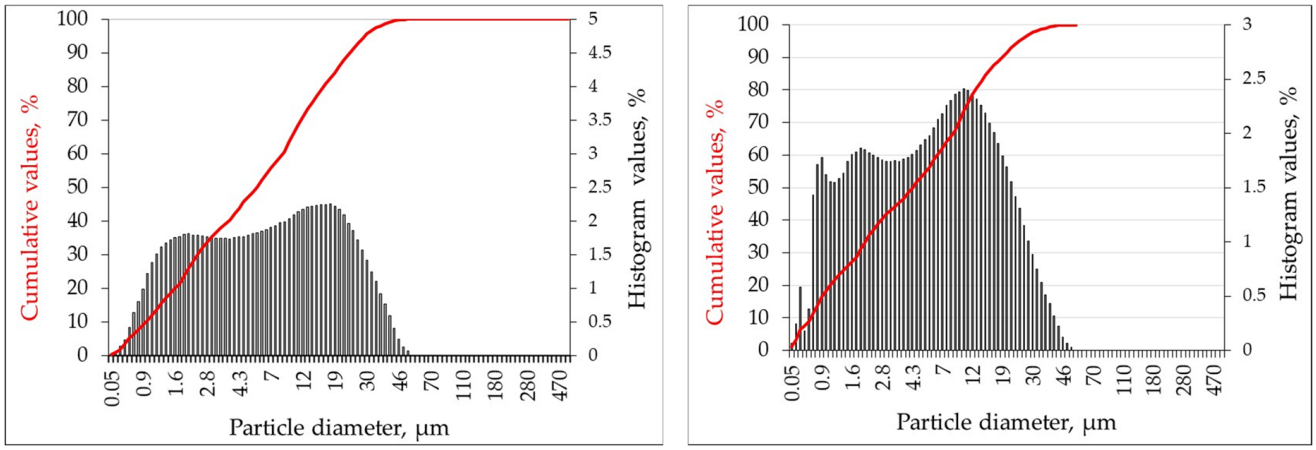

(**a**) (**b**)

Figure 1. Particle size distribution of raw materials: (**a**) OPC (absolute density 3.03 kg/m^3); (**b**) PG (absolute density 2.52 kg/m^3).

Surface area measurements (Blaine method) indicated that PG particles (208 m^2/g) were approximately 1.68 times coarser than OPC particles (350 m^2/g).

X-ray diffraction (XRD) analysis (see Figure 2) revealed that the mineral composition of phosphogypsum (PG) is dominated by basanite, with minor occurrences of brushite. This finding aligns with the mineralogical characteristics reported by Fornes et al. [23].

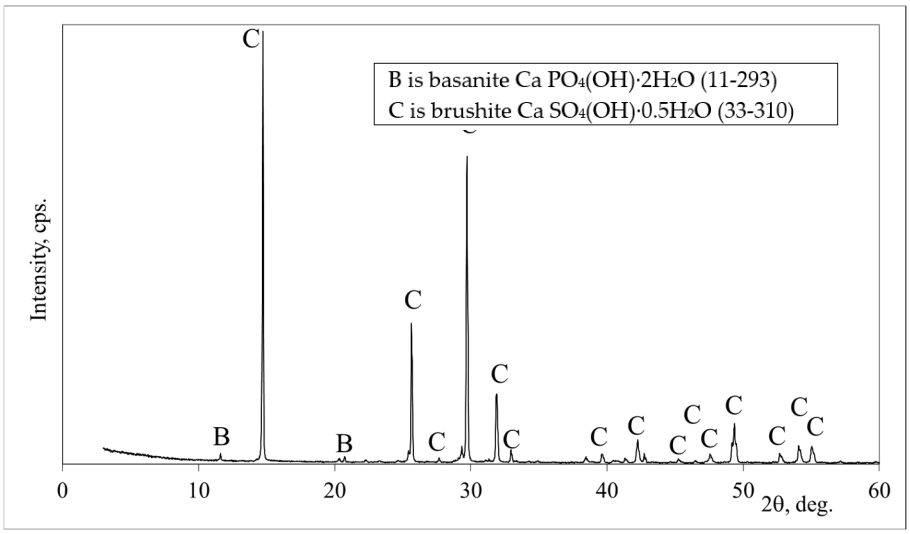

Figure 2. Mineral composition of phosphogypsum, determined by X-ray diffraction (XRD).

Scanning electron microscopy (SEM) observations (see Figure 3) further indicated that PG particles predominantly exhibit prismatic morphologies.

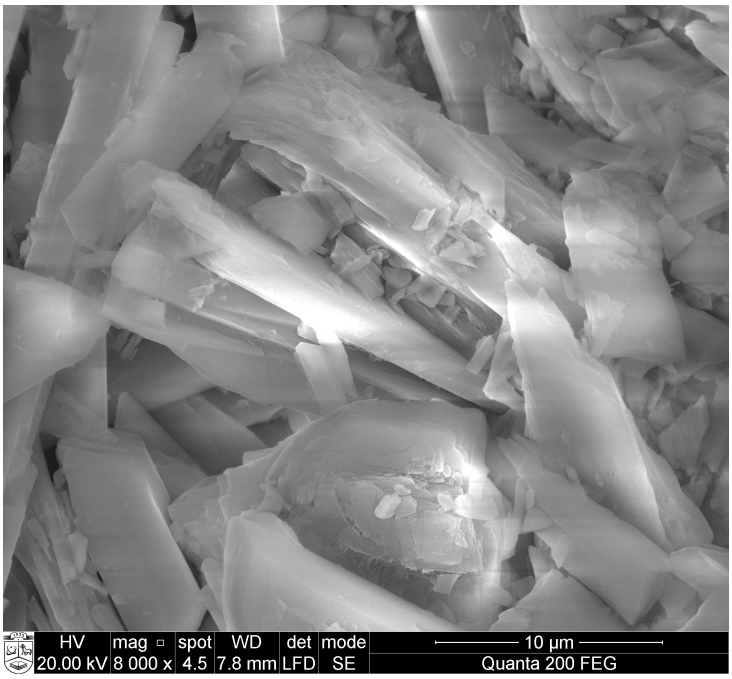

Figure 3. Microstructure of phosphogypsum, observed through scanning electron microscopy (SEM).

Natural sand was employed as the fine aggregate in the preparation of OPC-based mortar (fine-grained concrete). The sand used was clean and free from clay, silt, and organic contaminants, exhibiting a water absorption of 0.55%. Although the sand initially contained moisture, it was oven-dried at 100 °C in the laboratory until a constant mass was achieved to minimize the water-to-sand ratio in the mix. The particle size fraction of the sand ranged from 0 to 8 mm, and its granulometric distribution is presented in Figure 4.

In addition, a polycarboxylate-based superplasticizer was incorporated into the mixtures to enhance workability and achieve the desired consistency.

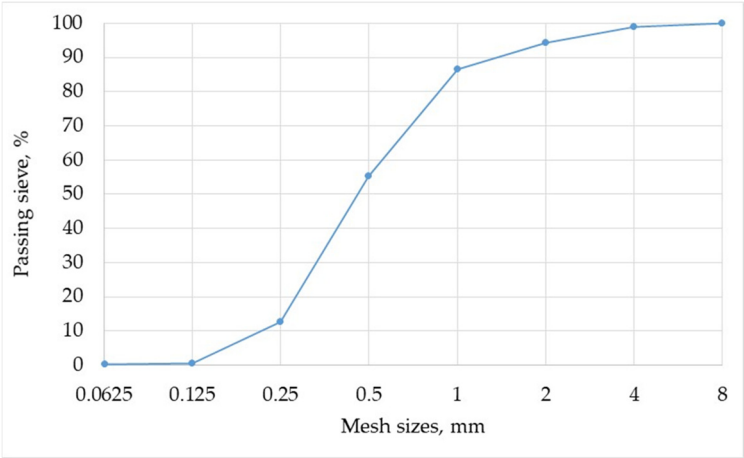

Figure 4. Granulometric composition of sand aggregate.

2.2. Preparation of Forming Mixtures

The composition of the initial materials for OPC-based mortar is shown in Table 2. Six types of OPC-based mortars samples were prepared. Reference samples were made from OPC powder, superplasticizer, sand, and water. The PG powder was used to replace a portion of the OPC in the remaining samples. The same ratio of water-to-OPC was used in all of the samples. The PG content was calculated based on the mass of OPC and set at 0, 3, 6, 9, 12, and 15%. Accordingly, the samples were designated as PG-0 through PG-15 (Table 2).

Table 2. Composition of mixtures of ordinary Portland cement-based mortar, g.

Samples	OPC	PG	Superplasticizer	Sand	Water-to-OPC + PG Ratio (W/S)
PG-0	522.0	0.0	5.2	1565.0	0.500
PG-3	506.3	15.7	5.2	1565.0	0.500
PG-6	490.6	31.4	5.2	1565.0	0.500
PG-9	475.0	47.0	5.2	1565.0	0.500
PG-12	459.4	62.6	5.2	1565.0	0.500
PG-15	443.7	78.3	5.2	1565.0	0.500

The mortar mixtures of different compositions were mixed in a "E095" mixer of 5 L capacity in the following order. Portland cement and sand were dry mixed together for 2 min (the speed of the mixer's working shaft was 62 rpm). Then, the required amount of water was added to the mortar mixture and additionally wet-mixed for 1 min (the speed of the mixer's working shaft was also 62 rpm). After that, the speed of the mixer's working shaft was increased to 140 rpm and the mixing procedure was continued for another 3 min. The prepared mortar mixtures were poured into the prism-shaped steel molds (40 × 40 × 160 mm) and compacted on a vibrating table for 20 s. The compacted mortar mixtures were cured in steel molds, which were placed in the climatic chamber (relative humidity 65 ± 5%, temperature 20 ± 2 °C) for 2 days. After that, the hardened mortar samples were removed from the steel molds and kept in the same climatic chamber (relative

humidity 65 ± 5%, temperature 20 ± 2 °C) for a number of days until the measurements were made.

2.3. Test Methods

Initial materials and hardened samples were analyzed using the following methods.

X-ray fluorescence analysis (XRF): Before analysis, the samples were ground at a speed of 950 rpm in a Pulverisette 9 (Fritsch GmbH, Idar-Oberstein, Germany) vibratory disk mill and sieved through a sieve with a mesh size of 40 µm. Then, 9 g of the ground samples was weighed, mixed with 1 g of methylcellulose tablets, and ground again for 3 min at a speed of 950 rpm. The ground samples were pressed into tablets using a load of ~20 MPa. XRF was performed using an S8 Tiger WD X-ray fluorescence spectrometer (Bruker AXS GmbH, Karlsruhe, Germany). A rhodium (Rh) tube was used with an anode voltage of Ua up to 60 kV and a current intensity of I up to 130 mA. The pressed samples were measured in a helium atmosphere. The measurements were performed using the Spectra Plus Quant Express method.

X-ray diffraction analysis (XRD) was performed using a D8 Advance diffractometer (Bruker AXS GmbH, Karlsruhe, Germany). The following were used: radiation—CuKα, filter—Ni, detector movement step 0.02°, intensity measurement duration per step—0.2 s, anode voltage Ua = 40 kV, current intensity I = 40 mA. The accuracy of X-ray diffraction analysis measurements was 2θ = 0.01°.

The laboratory equipment was a CILAS 1090 LD (3P Instruments GmbH & Co., Odelzhausen, Germany) laser scattering particle size analyzer.

Hydration temperatures of the cement paste were measured using the semi-adiabatic calorimetry method in accordance with EN 196-9:2010 [24]. The temperature development was recorded with an 8-channel USB TC-08 data logger equipped with a K-type thermocouple, capable of measuring temperatures in the range of −270 °C to +1820 °C.

The flexural and compressive strengths of hardened (after 7, 28, and 90 days) mortar samples were determined according to the requirements of the standard EN 1015-11:2019. An electromechanical testing machine H200 kU (Tinius Olsen, Orlando, FL, USA) was used, with a load capacity of 200 kN and a load measurement error of ± 0.5%. The flexural strength from 3 prism-shaped samples of each mortar mixture were tested. Three-point bending was used in the test. The applied load was 40 N/s. The compressive strength from 6 samples of each mortar mixture were tested. The prism halves, which remained after the flexural strength experiment, were used. The applied load was 400 N/s.

Thermal analysis (DTA/TG) was conducted to assess the influence of phosphogypsum (PG) dosage on the formation of hydration products in hardened OPC paste. The tests were performed using a STA PT-1600 (Linseis Messgeraete GmbH, Selb, Germany) thermal analyzer under the following conditions: heating rate of 10 °C·min^{-1}, temperature range of 30–1000 °C, empty platinum crucible as the reference, and nitrogen (N_2) as the furnace atmosphere.

The porosity parameters of the samples were evaluated using water absorption kinetics according to GOST 12730.4-78 [25], which defines open porosity (capillary pores), total porosity, and closed porosity (air pores).

3. Results and Discussion

The influence of phosphogypsum (PG) on the hydration temperature of OPC paste was assessed using semi-adiabatic calorimetry (see Figure 5). The results show that PG addition alters the heat evolution profile during hydration, indicating changes in reaction kinetics and phase formation. While PG does not significantly affect the overall hydration duration, the presence of sulfate ions promotes the formation of ettringite and other sulfate-

bearing phases. This effect is evident in the initial temperature rise, increasing from 40.5 °C for the reference sample to 43.4 °C for the PG-6 mixture. However, further increasing the PG content (9%, 12%, and 15%) resulted in a gradual decrease in hydration temperature to 42.5 °C and 41.6 °C for the PG-9, PG-12, and PG-15 samples, respectively. This reduction is likely due to the dilution effect of OPC at higher PG levels.

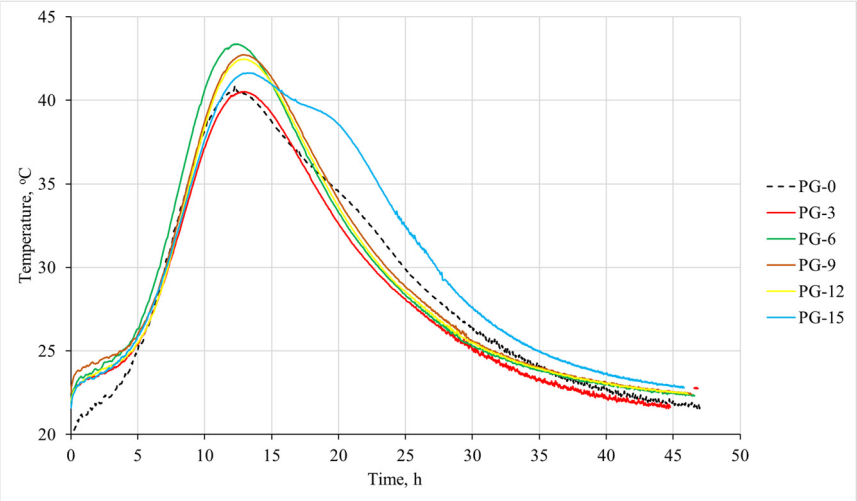

Figure 5. The influence of phosphogypsum additive on the hydration temperature of OPC paste, based on calorimetry results.

In OPC systems, PG introduces additional sulfate ions that react with C_3A to form ettringite early in the hydration process [26]. This initial reaction often results in a higher temperature release peak compared to plain OPC. Consequently, PG-modified pastes typically exhibit elevated hydration temperatures, reflecting intensified early-stage reactions. These findings were approved by Wolf et al. [27], who stated that rapid ettringite formation in OPC-rich mixes leads to high early heat release.

Sulfate balance refers to the proper proportion of sulfate ions needed to regulate the reactions between C_3A, C_3S, and the associated calcium aluminate hydrates, ensuring controlled hydration and appropriate mineralogical development. During the first 24 h of hydration in Portland cement-based binders, sulfate is progressively consumed through the formation of ettringite and early C–S–H, which together govern the kinetics of both aluminate and silicate reactions. The calorimetry results (Figure 5) reveal that PG addition modifies hydration kinetics by influencing early sulphate reactions and heat evolution. These trends confirm that PG alters the timing and intensity of hydration events, which is critical for controlling setting behavior and dimensional stability. This observation aligns with sulphate balance principles discussed by Canbek et al. [28], who emphasized the importance of managing sulphate availability to optimize hydration reactions in blended systems.

PG $\leq$ 6% slightly advances/intensifies early reactions (C_3S peak around 14.8 h), consistent with accelerated ettringite formation due to additional sulfates (Table 3). PG $\geq$ 9% shifts the main peak to later times (≈17–18 h), reflecting clinker dilution and slower silicate hydration. The sulfate depletion and aluminate shoulder occur ≈ 8 h after the main peak across mixes, which is consistent with the textbook picture that the post-peak shoulder arises from renewed C_3A reaction after sulfate in solution is depleted [29].

Table 3. Timing of main hydration events, hours.

Samples	C_3S Peak	Sulfate Depletion (First Local min of Dt/dt After C_3S)	C_3A Peak (Next Local Max)
PG-0	13.87	20.70	20.90
PG-3	16.60	24.30	24.57
PG-6	14.80	22.77	22.77
PG-9	17.17	25.13	25.13
PG-12	17.80	25.73	25.77
PG-15	17.40	25.37	25.37

The effect of PG on strength development is illustrated in Figure 6. The incorporation of phosphogypsum as an expansive agent resulted in a noticeable reduction in mechanical strength. Increasing PG content within the OPC system led to a progressive decline in both flexural and compressive strength. The reference sample without PG addition exhibited a flexural strength of 7.2 MPa, whereas the mixture containing 15% PG showed a reduced value of 4.6 MPa, corresponding to a 38% decrease. A similar trend was observed for compressive strength, where the reduction was even more pronounced, reaching approximately 47%.

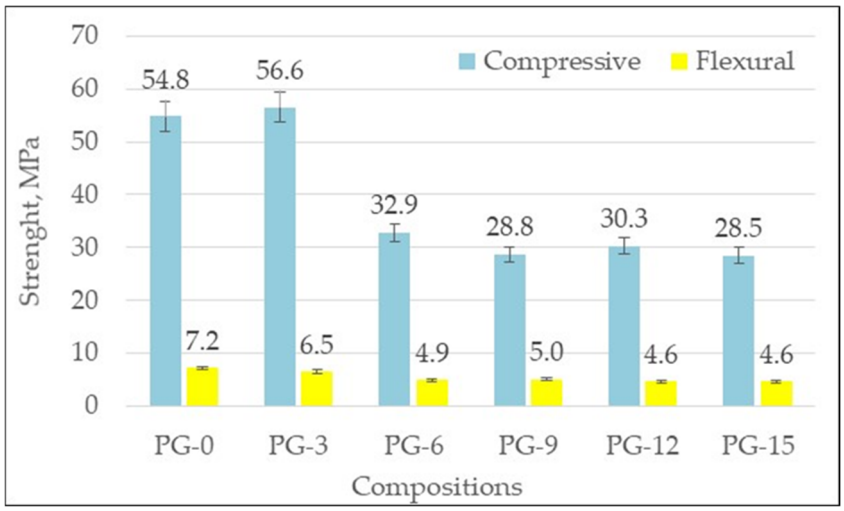

Figure 6. Influence of phosphogypsum additive on compressive and flexural strengths of the OPC-based mortar.

This strength loss can be attributed to several factors. First, the dilution effect caused by replacing part of OPC with PG reduces the amount of reactive clinker phases, limiting the formation of strength-contributing hydration products such as C–S–H. Second, the presence of excess sulfate ions promotes extensive ettringite formation, which, while beneficial for shrinkage mitigation, can lead to microstructural weaknesses when formed in large quantities. At higher PG contents, unreacted gypsum may remain in the matrix, further compromising the integrity of the hardened paste. Islam et al. [30] investigated the effect of phosphogypsum (PG) addition (2–15%) on the mechanical strength of OPC materials and reported that higher PG content significantly reduces compressive strength. This reduction is primarily attributed to the dilution effect, which lowers the proportion of reactive clinker phases, and the presence of excess sulfate ions, which promote extensive ettringite formation. Gyabaah et al. [31] demonstrated that excessive ettringite formation can weaken the matrix and reduce long-term strength. Increasing SO_3 content from gypsum reduced

long-term strength due to microstructural changes and excessive ettringite formation. Ait Brahim et al. [32] observed that phosphogypsum additions exceeding 10% decrease compressive strength because unreacted gypsum remains in the matrix, compromising microstructural integrity.

Using the ANOVA methodology, it was determined that the amount of phosphogypsum (PG) in the samples does not have a statistically significant effect on either the compressive strength or flexural strength. In both cases, the calculated Fisher test values (F) (see Tables 4 and 5)—1.92 and 0.74, respectively—are substantially lower than the critical value (Fcrit = 4.96).

Table 4. Single-factor ANOVA results for the amount of PG on compressive strength of OPC mortars.

SUMMARY						
Groups	**Count**		**Sum**	**Average**		**Variance**
Compressive strength, MPa	6		139.903	23.317		751.040
PG, %	6		45	7.5		31.5
ANOVA						
Source of variation	Sum of squares (SS)	Degree of freedom (df)	Mean square (MS)	F-statistic (F)	Probability (p-value)	Critical F (Fcrit)
Between Groups	750.55	1	750.55	1.92	0.196	4.96
Within Groups	3912.70	10	3912.70			
Total	4663.25	11				

Table 5. Single-factor ANOVA results for the amount of PG on flexural strength of OPC mortars.

SUMMARY						
Groups	**Count**		**Sum**	**Average**		**Variance**
Flexural strength, MPa	6		32.933	5.489		1.186
PG, %	6		45	7.5		31.5
ANOVA						
Source of variation	Sum of squares (SS)	Degree of freedom (df)	Mean square (MS)	F-statistic (F)	Probability (p-value)	Critical F (Fcrit)
Between Groups	12.134	1	12.134	0.74	0.409	4.96
Within Groups	163.430	10	16.343			
Total	175.564	11				

Despite the monotonic decline in strength with increasing PG content (Figure 6), the single-factor ANOVA did not indicate a statistically significant effect of PG on compressive ($F(1, 10) = 1.92$, $p = 0.196$, $\eta^2 = 0.161$, $\omega^2 = 0.071$) or flexural strength ($F(1, 10) = 0.74$, $p = 0.409$, $\eta^2 = 0.069$, $\omega^2 \approx 0$) at $\alpha = 0.05$.

Although the mean values showed a decreasing tendency, the variability within groups limited statistical significance. For compressive strength, a slight initial increase was observed (3% of PG), but when the PG content exceeded 6%, the strength values stabilized within the range of 28.53–32.86 MPa. A similar pattern was evident for flexural strength: incorporating 3% PG reduced the strength from 7.2 MPa to 6.5 MPa, and at PG contents above 6%, flexural strength remained in the range of 4.6–5.0 MPa (Figure 6). This indicates

that, while higher PG dosages tended to lower strength, the observed differences were not statistically significant based on the ANOVA results.

Figure 7 presents the X-ray diffraction (XRD) analysis of hardened cement paste with phosphogypsum additive at 28 days of hydration revealed a diverse mineralogical composition, including portlandite ($Ca(OH)_2$), calcite ($CaCO_3$), and ettringite ($Ca_6Al_2(SO_4)_3(OH)_{12}\cdot 26H_2O$), and residual clinker phases such as alite and larnite, calcium silicate hydrate (C-S-H), brownmillerite, and traces of gypsum.

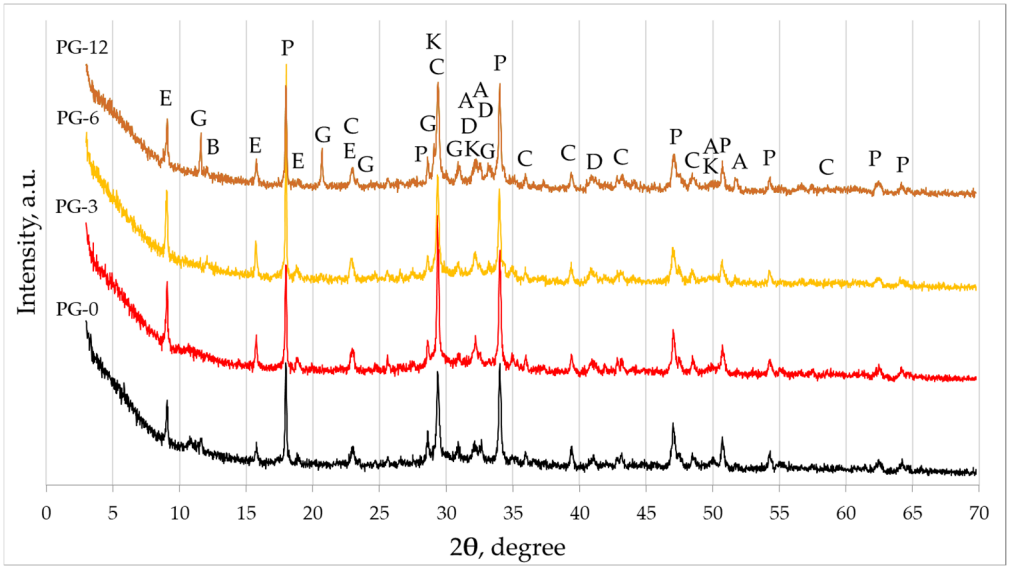

Figure 7. Mineral composition of hardened cement pastes with phosphogypsum additive at 28 days of hydration, according to X-ray diffraction (XRD) analysis. Notes: P—portlandite $Ca(OH)_2$ (44-1481); C—calcite $CaCO_3$ (5-586); E—ettringite $Ca_6Al_2(SO_4)_3(OH)_{12}\cdot 26H_2O$ (41-1451); A—alite $Ca_{54}MgAl_2Si1_6O_{90}$ (13-272); D—larnite $Ca_2(SiO_4)$ (83-461); K—calcium silicate hydrate $Ca_{1.5}SiO_{3.5}\cdot xH_2O$ (33-306); B—brownmillerite $Ca_2(Al,Fe)_2O_5$ (30-226), G—gypsum $CaSO_4\cdot 2H_2O$ (33-311).

The presence of ettringite and gypsum indicates active sulfate interaction from phosphogypsum, which promotes secondary hydration reactions and potentially enhances dimensional stability. In contrast, the OPC paste without phosphogypsum primarily exhibited portlandite, calcite, C-S-H, and residual clinker phases, with significantly lower ettringite content and no detectable gypsum. This difference suggests that phosphogypsum contributes additional sulfate ions, accelerating ettringite formation and influencing the microstructure and strength of the hardened paste. Including up to 6% of PG led to a slight increase in the peaks of ettringite, and the inclusion of PG at higher amounts (FG-12) resulted in some gypsum remaining unreacted in the system. In a similar study, Ait Brahim et al. [32] reported that OPC modified with 0–15% phosphogypsum exhibited hydration products such as ettringite, C-S-H, portlandite, and calcite, as confirmed by XRD analysis.

Figure 8 presents the DTA/TG curves for cement pastes with different phosphogypsum (PG) contents (0%, 3%, 6%, 12%), allowing for a direct comparison of thermal decomposition behavior at 28 days. The curves illustrate how increasing PG content influences dehydration, decarbonization reactions, sulfate-related phase transformations, and mass-loss trends in the system.

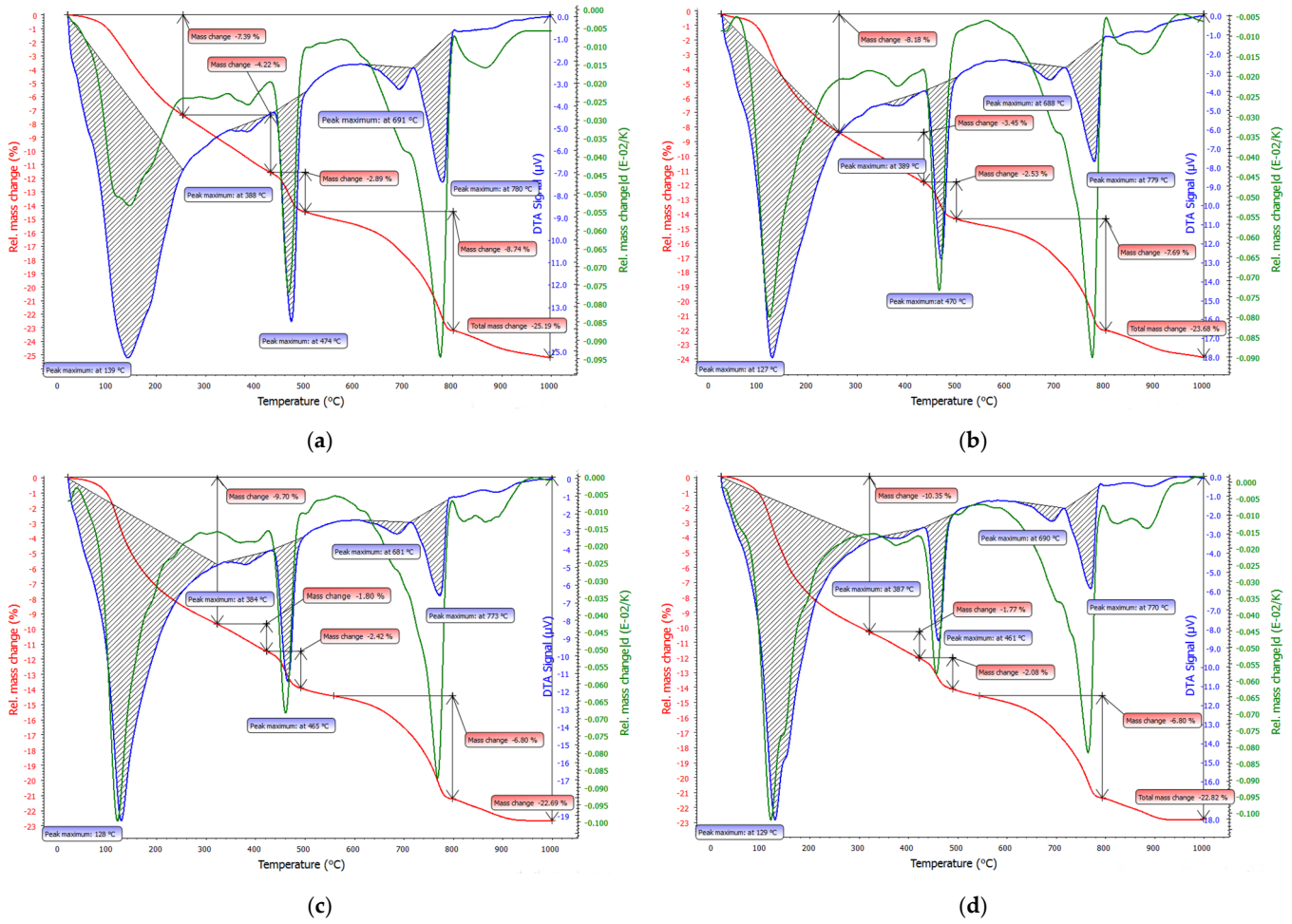

Figure 8. Thermal analysis (DSC/TG) of hardened cement pastes with phosphogypsum additive after 28 days of hydration: (**a**) PG-0 sample without PG; (**b**) PG-3 sample with 3% PG; (**c**) PG-6 sample with 6% PG; and (**d**) PG-12 sample with 12% PG.

In all samples, the first broad endothermic peak (≈30–260 °C) corresponds to the loss of physically and chemically bound water from C–S–H-type gels and other early hydration products such as ettringite. The intensity of this peak increases progressively from PG-0 to PG-12, indicating that higher PG content promotes greater formation of hydration products capable of binding water. He et al. [33] reported that about 50% of the non-evaporable water in C–S–H is removed below 200 °C, confirming that the dehydration of physically and chemically bound water occurs within this temperature range. This first peak (Figure 8) corresponds to the decomposition of ettringite as well, which typically occurs between 25 and 130 °C [34]. In this case, however, it is not possible to quantify the ettringite content, as no distinct, non-overlapping peaks are observed within this temperature range.

The second major endothermic peak corresponds to the dehydroxylation of portlandite ($Ca(OH)_2$), which typically occurs within the 430–500 °C temperature range. This transformation involves the breakdown of $Ca(OH)_2$ into CaO and H_2O, representing the principal mass-loss stage associated with portlandite decomposition. This temperature interval corresponds to the well-known dehydroxylation range of portlandite in cementitious materials [35]. The mass loss related to this interval constantly decreases by increasing the amount of PG in the system (Table 6). This trend is attributed to a dilution effect, where PG partially replaces OPC and consequently reduces portlandite formation. Consequently, the calculated $Ca(OH)_2$ content decreases from 11.89 wt% in the reference sample (0% PG) to 8.55 wt% when 15% PG is incorporated.

Table 6. Results of thermogravimetric analysis for hardened cement paste after 28 days.

Samples	Mass Loss, wt% at Specific Temperatures			
	≈30–260 °C	430–500 °C	540–800 °C	30–1000 °C
PG-0	7.39	2.89	8.77	25.19
PG-3	8.18	2.59	7.69	23.68
PG-6	9.70	2.42	6.80	22.69
PG-12	10.35	2.08	6.80	22.82

The third major endothermic peak in the high-temperature region (540–800 °C) corresponds to the decarbonation of $CaCO_3$ [36]. The associated mass loss gradually decreases with increasing PG content, indicating a lower degree of carbonation in PG-modified samples. This behavior can be explained by a dilution effect: incorporating PG reduces the proportion of OPC in the blend, thereby decreasing portlandite formation during hydration. With less $Ca(OH)_2$ available, the subsequent conversion of portlandite to calcite during carbonation is also reduced, resulting in lower $CaCO_3$ decarbonation mass loss.

Shrinkage deformation is one of the most critical challenges affecting the durability and structural performance of ordinary Portland cement (OPC) concrete. Excessive shrinkage can lead to cracking, reduced mechanical integrity, and long-term deterioration, especially in large-scale or restrained structural elements. As the demand for sustainable and high-performance construction materials grows, researchers are exploring alternative additives that can mitigate shrinkage while enhancing other concrete properties. The results of drying shrinkage measurements for OPC-based mortars are presented in Figure 9.

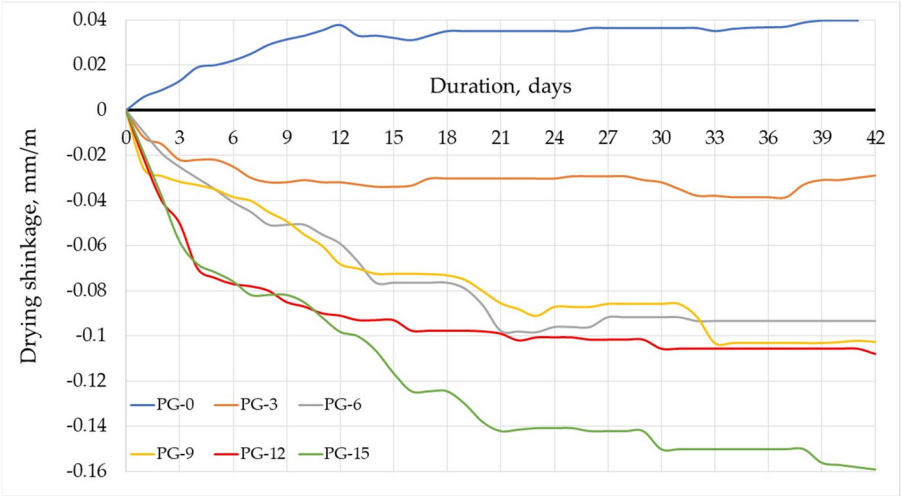

Figure 9. Influence of phosphogypsum additive on drying shrinkage of OPC-based mortars.

The reference sample (PG-0), composed of 100% OPC as the binder, exhibited the highest 43-day drying shrinkage of 0.0397 mm/m. The incorporation of PG significantly modified the shrinkage behavior. Mixtures with increasing PG content (PG-3, PG-6, PG-9, PG-12, and F15) demonstrated markedly lower drying shrinkages of −0.0230, −0.0933, −0.1030, −0.1104, and −0.1600 mm/m, respectively. This reduction in shrinkage in OPC-based mortars can be attributed to the formation of ettringite, a calcium sulfoaluminate hydrate, during the early hydration process. Sulfate ions from gypsum or PG react with aluminates in OPC to form ettringite, which occupies a larger volume than the original reactants, generating a slight expansive effect that counteracts drying shrinkage. Additionally, ettringite crystals grow within the capillary pores, refining the pore structure and creating

a denser matrix. This microstructural refinement reduces water loss during drying, thereby limiting evaporation and maintaining internal moisture, which stabilizes the material's volume and further mitigates shrinkage. Furthermore, at higher PG levels (12% and 15%), some gypsum ($CaSO_4 \cdot 2H_2O$) remained unreacted, which also contributed to shrinkage reduction but negatively impacted strength properties (see Figure 6). Similar results related to the pore-refining behavior of ettringite were published another study. Zheng et al. [37] reported that, in alkali-activated fly ash/slag mortars, the reduction in shrinkage achieved by incorporating 5% PG is primarily attributed to the formation of ettringite, which refines the pore structure. Liu et al. [38] reported that incorporating PG into ultra-high-performance concrete effectively reduces early-age shrinkage. Shrinkage curves reveal slight elongation in PG-containing mixtures, attributed to continuous ettringite formation from excess sulfate ions. Overall, higher PG content significantly mitigates autogenous shrinkage, enhances durability, and contributes to the long-term structural performance of this type of concrete.

The thermal analysis results provide an explanation for the measured reduction in the shrinkage of PG-modified cement pastes. The progressive increase in the low-temperature dehydration peak (≈30–260 °C) with rising PG content indicates greater formation of bound-water-rich hydrates such as C–S–H and ettringite, which refine the pore structure and reduce capillary stresses, thereby lowering drying shrinkage. These thermal signatures show that PG shifts the hydration pathway toward phases that densify the matrix and bind more water while limiting portlandite and calcite formation, directly correlating with the substantial shrinkage reduction observed in the PG-modified mixes.

Porosity parameters were obtained from water absorption kinetics in accordance with GOST 12730.4, which derives total, open, and closed porosity from density and water absorption measurements and characterizes pore size indicators from the absorption–time curves. The durability assessment of OPC mortars modified with PG (Table 7) shows that increasing PG content led to a gradual rise in water absorption and total porosity, accompanied by a reduction in the frost resistance factor K_F. This trend indicates that higher PG dosages tend to generate a more open pore structure, particularly an increase in interconnected open porosity (Pa), which is known to intensify moisture transport and consequently reduce freeze–thaw stability. Although closed porosity (Pu) remained relatively stable across all mixtures, the rise in open porosity from 18.15% (PG-0) to 22.19% (PG-15) contributed to a decrease in K_F from 2.14 to 1.77, resulting in a lower predicted number of cycles. Nevertheless, all mortars demonstrated medium to high frost resistance, with expected durability ranging from approximately 300 to 450 freeze–thaw cycles. This suggests that, despite the slight deterioration in microstructural compactness caused by higher PG inclusion, the overall structural integrity of the hardened matrix remained sufficient to ensure acceptable resistance to cyclic freezing. The results highlight that moderate PG contents (<6%) do not severely compromise durability, whereas higher dosages (>9–12%) may increase porosity to a level where frost resistance begins to decline more noticeably.

In conclusion, phosphogypsum shows strong potential as a shrinkage-reducing additive for sustainable construction, with low dosages effectively enhancing hydration, promoting ettringite formation, refining pore structure, and significantly reducing shrinkage. However, higher PG levels introduce clinker dilution and residual gypsum, leading to reduced mechanical performance. Thus, optimizing the PG replacement level is essential to balance shrinkage control, strength, and sustainability benefits.

Table 7. Results of durability parameters of hardened OPC mortar after 28 days.

Samples	Water Adsorption, %	Total Porosity, %	Open Porosity Pa, %	Closed Porosity Pu, %	Frost Resistance Factor, K_F	Predicted Cycles
PG-0	8.61	21.65	18.15	3.50	2.14	~420–450
PG-3	8.80	22.91	19.32	3.59	2.07	~400–430
PG-6	9.32	21.57	18.56	3.02	1.81	~330–360
PG-9	10.62	23.95	20.60	3.23	1.74	~310–340
PG-12	10.77	25.66	22.10	3.63	1.83	~340–370
PG-15	11.11	25.72	22.19	3.53	1.77	~320–350

4. Conclusions

- Low PG additions ($\leq$6%) slightly increase the hydration peak temperature, supporting early strength development. Higher PG contents (>9%) reduce the hydration peak due to clinker dilution and the presence of unreacted gypsum.
- Strength decreases sharply with increasing PG: at 15% PG, flexural strength drops by 38% and compressive strength by 47%. Reductions are attributed to clinker dilution, excess ettringite formation, and residual unreacted gypsum at high PG levels.
- According to phase evolution (XRD/TG–DTA), PG promotes ettringite formation at low dosages, while high PG contents leave unreacted gypsum. Increasing PG enhances low-temperature dehydration but reduces portlandite dehydroxylation ($Ca(OH)_2$) and $CaCO_3$ decarbonation, consistent with a dilution effect and lower Ca-bearing phase formation. $Ca(OH)_2$ content decreases from 11.89 wt% (0% PG) to 8.55 wt% (15% PG), confirming reduced portlandite formation and carbonation potential.
- Shrinkage improves significantly—from 0.0397 mm/m (reference) to -0.1600 mm/m at 15% PG—due to ettringite expansion and pore refinement. PG clearly enhances dimensional stability, but introduces a trade-off by lowering mechanical performance at higher replacement levels.
- Higher PG contents increase open porosity and water absorption, which gradually lowers the frost-resistance factor. Even so, all mortars retain medium–high durability ($\approx$300–450 cycles). Small PG additions (<6%) have minimal effects, whereas higher dosages (>9–12%) noticeably raise porosity and reduce freeze–thaw resistance.
- PG effectively reduces shrinkage and modifies hydration, pore structure, and thermal decomposition behavior. While beneficial for dimensional stability and sustainability, high PG replacement levels compromise strength, indicating the need for an optimized PG dosage balancing durability and mechanical performance.

5. Future Perspectives

Although this study demonstrates that phosphogypsum (PG) can effectively reduce drying shrinkage in OPC-based mortar while influencing hydration behavior and mechanical performance, several research directions remain open for further exploration. Future work should focus on optimizing PG dosage to balance shrinkage mitigation with mechanical strength. Advanced characterization techniques—such as SEM analysis—could provide deeper insights into the microstructural evolution of ettringite formation induced by PG. The interaction between PG and other supplementary cementitious materials (SCMs), such as fly ash, slag, or calcined clays, also warrants examination to develop multi-component, low-carbon binders with controlled shrinkage and improved durability. From a practical standpoint, long-term performance under real environmental conditions—including freeze–thaw resistance, carbonation, sulfate attack, and restrained shrinkage behavior in

structural elements—should be evaluated. The environmental and economic impacts of large-scale PG valorization in construction materials should also be assessed through life-cycle analysis (LCA) and cost–benefit studies. Overall, expanding this research can contribute to the creation of more durable, sustainable, and resource-efficient cementitious materials, supporting the broader transition toward circular economy principles in the construction industry.

Author Contributions: Conceptualization, V.R., M.K. and G.G.; methodology, V.R., D.V. and G.G.; software, M.K.; validation, V.R., D.V. and A.A.; formal analysis, V.R. and D.V.; investigation, V.R., D.V. and G.G.; resources, M.K. and G.G.; data curation, V.R. and D.V.; writing—original draft preparation, V.R., D.V. and G.G.; writing—review and editing, V.R., D.V. and A.A.; visualization, V.R., D.V. and A.A.; supervision, M.K. and G.G.; project administration, M.K.; funding acquisition, M.K. All authors have read and agreed to the published version of the manuscript.

Funding: This research was funded by the project "Civil Engineering Research Centre" (agreement No. S-A-UEI-23-5, ŠMSM).

Data Availability Statement: The original contributions presented in the study are included in the article. Further inquiries can be directed to the corresponding author.

Acknowledgments: The authors want to thank SC "Lifosa" for the donation of the phosphogypsum additive, which was used in the experiments.

Conflicts of Interest: The authors declare no conflicts of interest.

List of Abbreviations and Acronyms

DTA	Differential Thermal Analysis
LOI	Loss on Ignition
OPC	Ordinary Portland Cement
PG	Phosphogypsum
SEM	Scanning Electron Microscopy
SRA	Shrinkage-Reducing Additive
W/S	Water-to-Binder Ratio
XRD	X-ray Diffraction
XRF	X-ray Fluorescence
LCA	Life-Cycle Analysis
SCMs	Supplementary Cementitious Materials
C-S-H	Calcium Silicate Hydrate

References

1. Wu, L.; Farzadnia, N.; Shi, C.; Zhang, Z.; Wang, H. Autogenous shrinkage of high performance concrete: A review. *Constr. Build. Mater.* **2017**, *149*, 62–75. [CrossRef]
2. Bacharz, M.; Bacharz, K.; Trąmpczyński, W. Impact of Early-Age Curing and Environmental Conditions on Shrinkage and Microcracking in Concrete. *Materials* **2025**, *18*, 3185. [CrossRef]
3. Dey, A.; Vastrad, A.V.; Bado, M.F.; Sokolov, A.; Kaklauskas, G. Long-term concrete shrinkage influence on the performance of reinforced concrete structures. *Materials* **2021**, *14*, 254. [CrossRef]
4. Statkauskas, M.; Grinys, A.; Vaičiukynienė, D. Investigation of concrete shrinkage reducing additives. *Materials* **2022**, *15*, 3407. [CrossRef] [PubMed]
5. Ge, H.; Sun, Z.; Lu, Z.; Yang, H.; Zhang, T.; He, N. Influence and mechanism analysis of different types of water reducing agents on volume shrinkage of cement mortar. *J. Build. Eng.* **2024**, *82*, 108204. [CrossRef]
6. Wang, T.; Gong, J.; Chen, B.; Gong, X.; Luo, H.; Zhang, Y.; Qu, Z. Effects of shrinkage reducing agent and expanded cement on UHPC fluidity, mechanical properties, and shrinkage performance. *Adv. Mater. Sci. Eng.* **2021**, *1*, 9045754. [CrossRef]
7. Aly, T.; Sanjayan, J.G. Shrinkage-cracking behavior of OPC-fiber concrete at early-age. *Mater. Struct.* **2010**, *43*, 755–764. [CrossRef]
8. Zuo, S.; Yuan, Q.; Huang, T.; Zhang, M.; Wu, Q. Rheological behaviour of low-heat Portland cement paste with MgO-based expansive agent and shrinkage reducing admixture. *Constr. Build. Mater.* **2021**, *304*, 124583. [CrossRef]

9. Takahashi, K.; Matsui, K.; Asamoto, S.; Sakamoto, N. Multiscale structural changes and drying shrinkage of Portland cement pastes: Effects of a fatty-alcohol-based shrinkage reducing agent. *Mater. Struct.* **2022**, *55*, 44. [CrossRef]
10. Wan, Z.; He, T.; Yang, R.; Ma, X. The effect of shrinkage-reducing agents on autogenous shrinkage and drying shrinkage of cement mortar with accelerator. *Mech. Time-Depend. Mater.* **2024**, *28*, 2121–2150. [CrossRef]
11. Zhang, N.; Yang, Q.; Li, D.; Yu, Y.; Jiang, X.; Xu, J. Autogenous and drying shrinkage properties of precast recycled aggregate concrete. *Case Stud. Constr. Mater.* **2025**, *22*, e04355. [CrossRef]
12. Tutkun, B.; Barlay, E.S.; Yalçınkaya, Ç.; Yazıcı, H. Effect of internal curing on shrinkage and cracking potential under autogenous and drying conditions. *Constr. Build. Mater.* **2023**, *409*, 134078. [CrossRef]
13. Al Moman, A.; Sundar, D.; Zeng, K.; Tatar, J.; Radlińska, A.; Rajabipour, F. Autogenous and drying shrinkage in Ultra-High-Performance Concrete (UHPC) and the effectiveness of internal curing. *Constr. Build. Mater.* **2025**, *464*, 140217. [CrossRef]
14. Zhu, H.; He, Y.; Ji, D.; Tang, J.; Li, C. Experimental research on the mechanical properties and autogenous shrinkage of precast members joint concrete. *Buildings* **2022**, *12*, 373. [CrossRef]
15. Al-Alusi, M.R.M.; Kurdi, N.H.; Al-Hadithi, A.I.; Hammad, A. An experimental investigation of the mechanical characteristics and drying shrinkage of a single-size expanded polystyrene lightweight concrete reinforced with waste plastic fibres. *Constr. Build. Mater.* **2024**, *415*, 135048. [CrossRef]
16. Hanjitsuwan, S.; Injorhor, B.; Phoo-ngernkham, T.; Damrongwiriyanupap, N.; Li, L.Y.; Sukontasukkul, P.; Chindaprasirt, P. Drying shrinkage, strength and microstructure of alkali-activated high-calcium fly ash using FGD-gypsum and dolomite as expansive additive. *Cem. Concr. Compos.* **2020**, *114*, 103760. [CrossRef]
17. Bakharev, T.; Sanjayan, J.G.; Cheng, Y.B. Effect of admixtures on properties of alkali-activated slag concrete. *Cem. Concr. Res.* **2000**, *30*, 1367–1374. [CrossRef]
18. Liu, J.; Hu, L.; Tang, L.; Zhang, E.Q.; Ren, J. Shrinkage behaviour, early hydration and hardened properties of sodium silicate activated slag incorporated with gypsum and cement. *Constr. Build. Mater.* **2020**, *248*, 118687. [CrossRef]
19. Sultonov, B.E.; Nodirov, A.A.; Xolmatov, D.S. Research of the composition of phosphogypsum produced during the extracting of phosphoric acid from ordinary phosphorite powder by the clinker method. *Chem. Sci. Int. J.* **2023**, *32*, 51–58. [CrossRef]
20. Nizevičienė, D.; Vaičiukynienė, D.; Michalik, B.; Bonczyk, M.; Vaitkevičius, V.; Jusas, V. The treatment of phosphogypsum with zeolite to use it in binding material. *Constr. Build. Mater.* **2018**, *180*, 134–142. [CrossRef]
21. Tan, H.; Zou, F.; Liu, M.; Ma, B.; Guo, Y.; Jian, S. Effect of the adsorbing behavior of phosphate retarders on hydration of cement paste. *J. Mater. Civ. Eng.* **2017**, *29*, 04017088. [CrossRef]
22. Shi, Y.; Cheng, L.; Tao, M.; Tong, S.; Yao, X.; Liu, Y. Using modified quartz sand for phosphate pollution control in cemented phosphogypsum (PG) backfill. *J. Clean. Prod.* **2021**, *283*, 124652. [CrossRef]
23. Fornes, I.V.; Vaičiukynienė, D.; Nizevičienė, D.; Doroševas, V. The improvement of the water-resistance of the phosphogypsum by adding waste metallurgical sludge. *J. Build. Eng.* **2021**, *43*, 102861. [CrossRef]
24. *EN 196-9:2010*; Methods of Testing Cement. Heat of Hydration. Semi-Adiabatic Method. European Committee for Standardization (CEN): Brussels, Belgium, 2010.
25. *GOST 12730.4-78*; Concretes. Methods of Determination of Porosity Parameters. International Standard: Moscow, Russia, 2007.
26. Yang, Y.; Zhang, Q.; Shu, X.; Wang, X.; Ran, Q. Influence of sulfates on formation of ettringite during early C3A hydration. *Materials* **2022**, *15*, 6934. [CrossRef]
27. Wolf, J.J.; Jansen, D.; Goetz-Neunhoeffer, F.; Neubauer, J. Mechanisms of early ettringite formation in ternary CSA–OPC–anhydrite systems. *Adv. Cem. Res.* **2019**, *31*, 195–204. [CrossRef]
28. Canbek, O.; Szeto, C.; Washburn, N.R.; Kurtis, K.E. A quantitative approach to determining sulfate balance for LC3. *Cement* **2023**, *12*, 100063. [CrossRef]
29. Zunino, F.; Scrivener, K. The reaction between metakaolin and limestone and its effect in porosity refinement and mechanical properties. *Cem. Concr. Res.* **2021**, *140*, 106307. [CrossRef]
30. Islam, G.S.; Chowdhury, F.H.; Raihan, M.T.; Amit, S.K.S.; Islam, M.R. Effect of phosphogypsum on the properties of Portland cement. *Procedia Eng.* **2017**, *171*, 744–751. [CrossRef]
31. Gyabaah, G.; Miyazawa, S.; Nito, N. Effects of gypsum and limestone powder on fresh properties and compressive strength of concrete containing ground granulated blast furnace slag under different curing temperatures. *Constr. Mater.* **2022**, *2*, 114–126. [CrossRef]
32. Ait Brahim, J.; Benkaddour, A.; El Abbassi, F.E.; Tamraoui, Y.; Achiou, B.; Haneklaus, N.; Mazouz, H.; Beniazza, R. Properties of modified Portland cement with purified phosphogypsum to produce alternative material for construction. *Chem. Afr.* **2025**, *8*, 2629–2640. [CrossRef]
33. He, Y.; Zheng, X.; Lü, L.; Yu, S.; Deng, G.; Hu, S. Dehydration characteristics of CSH with Ca/Si ratio 1.0 prepared via precipitation. *J. Wuhan Univ. Technol.-Mater. Sci. Ed.* **2018**, *33*, 619–624. [CrossRef]
34. Noor, L.; Rost, P.; Kirchberger, I.; Goetz-Neunhoeffer, F.; Ideker, J.H. Hygrothermal stability of ettringite in blended systems with CAC-OPC-CŠ. *Cem. Concr. Res.* **2024**, *184*, 107590. [CrossRef]

35. Pane, I.; Hansen, W. Investigation of blended cement hydration by isothermal calorimetry and thermal analysis. *Cem. Concr. Res.* **2005**, *35*, 1155–1164. [CrossRef]
36. Omrani, I.A.; Kapeluszna, E.; Szydłowski, J.; Kotwica, Ł.; Koniorczyk, M. Limestone calcined clay (LC^3) cement: Ice content profile and calcium carbonate reaction vs pore structure and mechanical properties development. *J. Build. Eng.* **2025**, *100*, 111762. [CrossRef]
37. Zheng, Y.; Xuan, D.; Shen, B.; Ma, K. Shrinkage mitigation of alkali-activated fly ash/slag mortar by using phosphogypsum waste. *Constr. Build. Mater.* **2023**, *375*, 130978. [CrossRef]
38. Liu, Z.; Qi, X.; Lv, Y.; Shui, Z. Application of phosphogypsum in ultra-high-performance concrete (UHPC) matrix for strength enhancement and shrinkage reduction. *Materials* **2025**, *18*, 1135. [CrossRef] [PubMed]

Disclaimer/Publisher's Note: The statements, opinions and data contained in all publications are solely those of the individual author(s) and contributor(s) and not of MDPI and/or the editor(s). MDPI and/or the editor(s) disclaim responsibility for any injury to people or property resulting from any ideas, methods, instructions or products referred to in the content.